## Supplemental Materials and Methods

### Reagents and antibodies

The following antibodies and reagents were used: α-bungarotoxin Alexa Fluor® 488 conjugate (B13422, Life Technologies, 1/1000), anti-synaptophysin (08-0130, Invitrogen, 1/5), anti-neurofilament 68 kDa (AB9568, Millipore, 1/750), anti-SNAP25 (HPA001830, Sigma, 1/500), anti-HA (901514, BioLegend, 1/2500), anti-β-catenin (610153, BD Biosciences, 1/1000), anti-phospho β-catenin (phospho T41 + S45) (ab38511, Abcam, 1/500); anti-β-actin (ab8227, Abcam, 1/3000); anti-GAPDH (ab9485, Abcam, 1/5000); anti-GFP (11814460001, Roche, 1/500); anti-Myc (2276S, Ozyme, 1/500). Dkk1, Sfrp4, Wnt3a, Wnt4 and Wnt11 proteins were purchased from R&D Systems. Polyclonal (1/500 for western blot) and monoclonal (1/200 for immunostaining) anti-Vangl2 have been previously described (Montcouquiol et al., 2006; Puvirajesinghe et al., 2016).

### Images acquisition and processing.

All images were collected on a microscope (model BX61; Olympus) equipped with a Fast 1394 Digital CCD FireWire camera or on a confocal laser scanning microscope (Zeiss LSM-710). The same laser power and parameter setting were applied to ensure fair comparison between WT and mutant muscles. Confocal images presented are single-projected image derived from overlaying each set of collected Z-stacks. For quantification of the AChR clusters number, volume and intensity, image stacks were quantified using the ImageJ (version 1.46m) plugin “3D object counter” (Bolte and Cordelières, 2006). The threshold intensity was set by visual inspection of AChR clusters, being the same between WT and mutant images. The endplate band width was defined by the distance between the two farthest AChR clusters from the main nerve trunk. Around 100 measurements regularly spaced and covering the entire diaphragm were taken. For presynaptic quantification, the number and length of primary and secondary branches were performed from at least 6 single-projected

images per genotype using ImageJ software. Primary and secondary branches were defined as axons that extended from the main nerve trunk (primary) or from the primary branches (secondary). For analyses of E14/E14.5 injected-embryos, since secondary branches were not fully differentiated, we quantified the mean axon length defined as the total length of the axons that extended from the nerve trunk. At least 4 diaphragms or 50 isolated muscle fibers of each genotype were analyzed and quantified. To evaluate ß-catenin translocation to nuclei in myotubes, image stacks corresponding to nuclei were used for quantification using the ImageJ intensity plot profile.

## Supplemental references

**Bolte, S. and Cordelières, F. P.** (2006). A guided tour into subcellular colocalization analysis in light microscopy. *J. Microsc.* **224**, 213–232.

**Montcouquiol, M., Sans, N., Huss, D., Kach, J., Dickman, J. D., Forge, A., Rachel, R. A., Copeland, N. G., Jenkins, N. A., Bogani, D., et al.** (2006). Asymmetric localization of Vangl2 and Fz3 indicate novel mechanisms for planar cell polarity in mammals. *J. Neurosci. Off. J. Soc. Neurosci.* **26**, 5265–5275.

**Puvirajesinghe, T. M., Bertucci, F., Jain, A., Scerbo, P., Belotti, E., Audebert, S., Sebbagh, M., Lopez, M., Brech, A., Finetti, P., et al.** (2016). Identification of p62/SQSTM1 as a component of non-canonical Wnt VANGL2-JNK signalling in breast cancer. *Nat. Commun.* **7**, 10318.

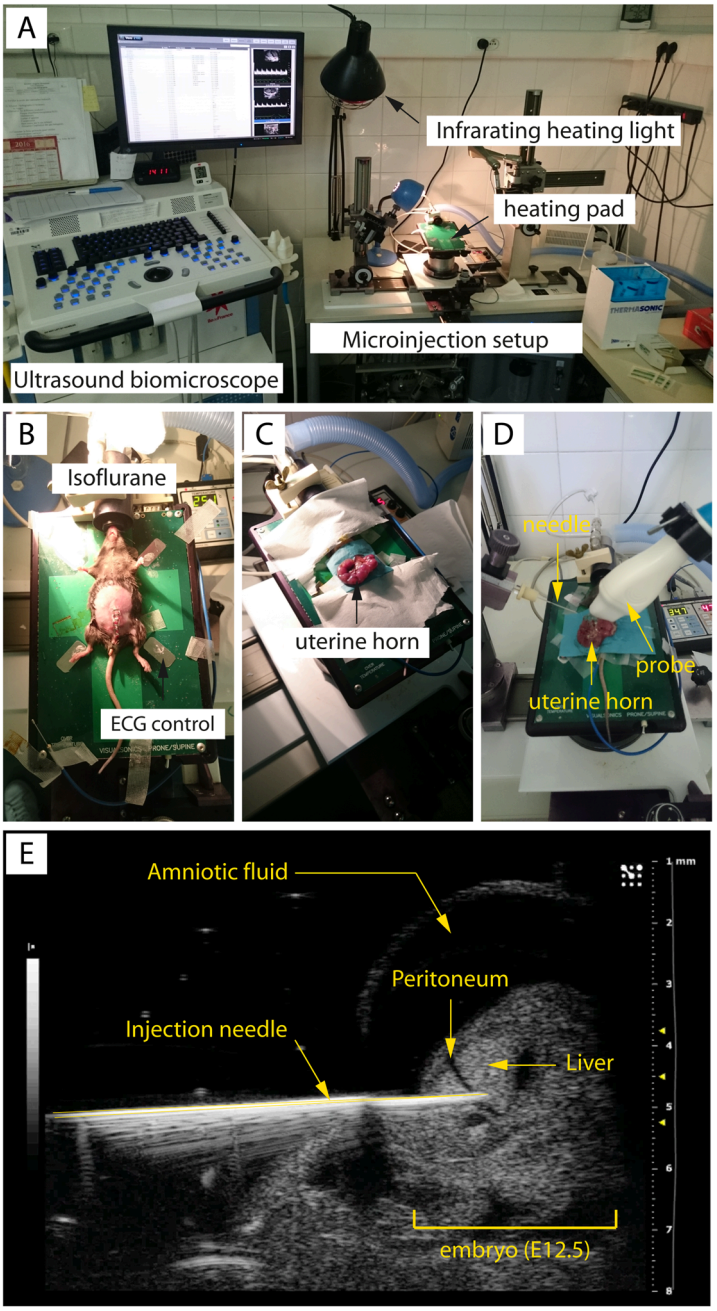


Figure S1.

**Figure S1. Setup for ultrasound-guided injections in live mice embryos.**

**(A)** Photography showing the heating pad on which the anesthetized pregnant mouse was installed and the ultrasound biomicroscope. Additional eating of the animal was ensured with an infrared eating light all along the experiment. **(B)** Monitoring respiration frequency, ECG and temperature of the mouse was performed. **(C)** A laparotomy was performed and the uterine horns were gently exteriorized. **(D)** A warm sterile gel was used to ensure contact between the ultrasound probe and the embryos (E12.5). Quartz micropipette for *in vitro*

fertilization was used to inject into the embryo together with the Visualsonics microinjection positioning system. **(E)** Example of an ultrasound image showing a microinjection performed directly in the embryo peritoneum. Note that the peritoneum is identified depending on the location of the liver.

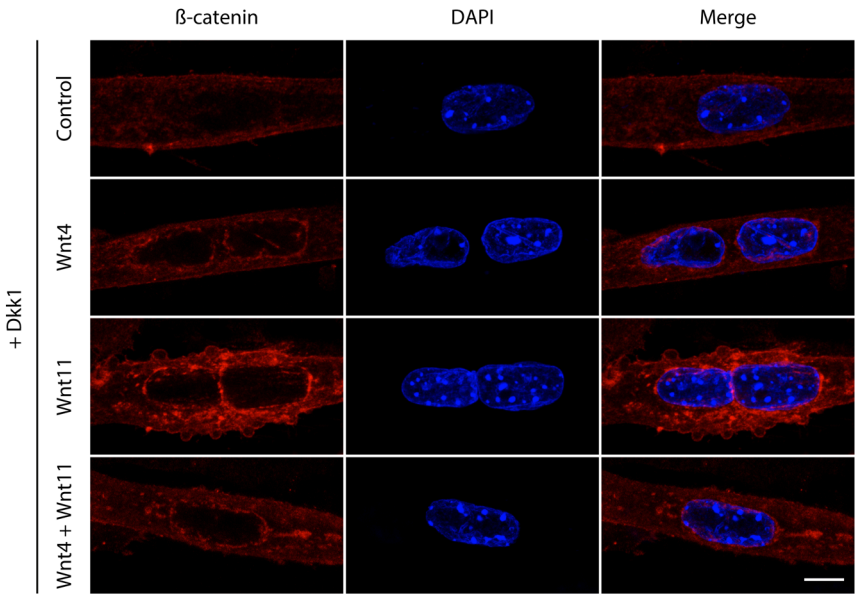


Figure S2.

**Figure S2. Dkk1 impairs β-catenin nuclear accumulation in myotubes treated with Wnt4 and/or Wnt11.**

Examples of myotubes stained with total β-catenin (red) together with DAPI (blue, nuclei) treated with Dkk1 (20 ng/ml) in the absence or presence of Wnt4 and/or Wnt11 (10 ng/ml). Scale bar in the merged image, 10 μm.

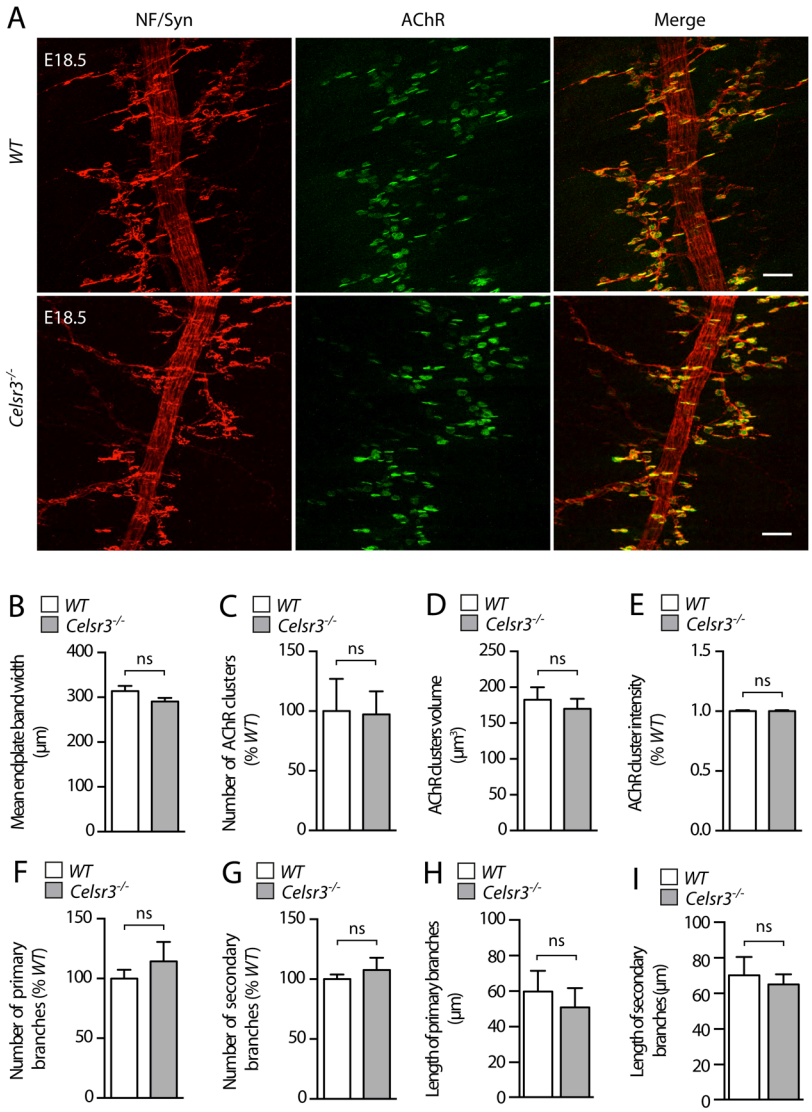


Figure S3.

**Figure S3. Celsr3 is dispensable for NMJ formation in diaphragms.**

**(A)** Confocal images of whole mount left hemidiaphragms from E18.5 *WT* and *Celsr3*$^{-/-}$ embryos stained with neurofilament (NF, red) and synaptophysin (Syn, red) antibodies together with α-BTX (AChRs, green). **(B-I)** Quantitative analysis of the endplate band width (B), the AChR clusters number (C), volume (D), fluorescence intensity (E), the number of primary (F) and secondary (G) nerve branches and the mean primary (H) and secondary (I) neurite length. Data are shown as mean ± SEM. ns, non significant. N = 5 embryos per genotype, Mann-Whitney U test. Scale bar in the merged image in A, 50 µm.

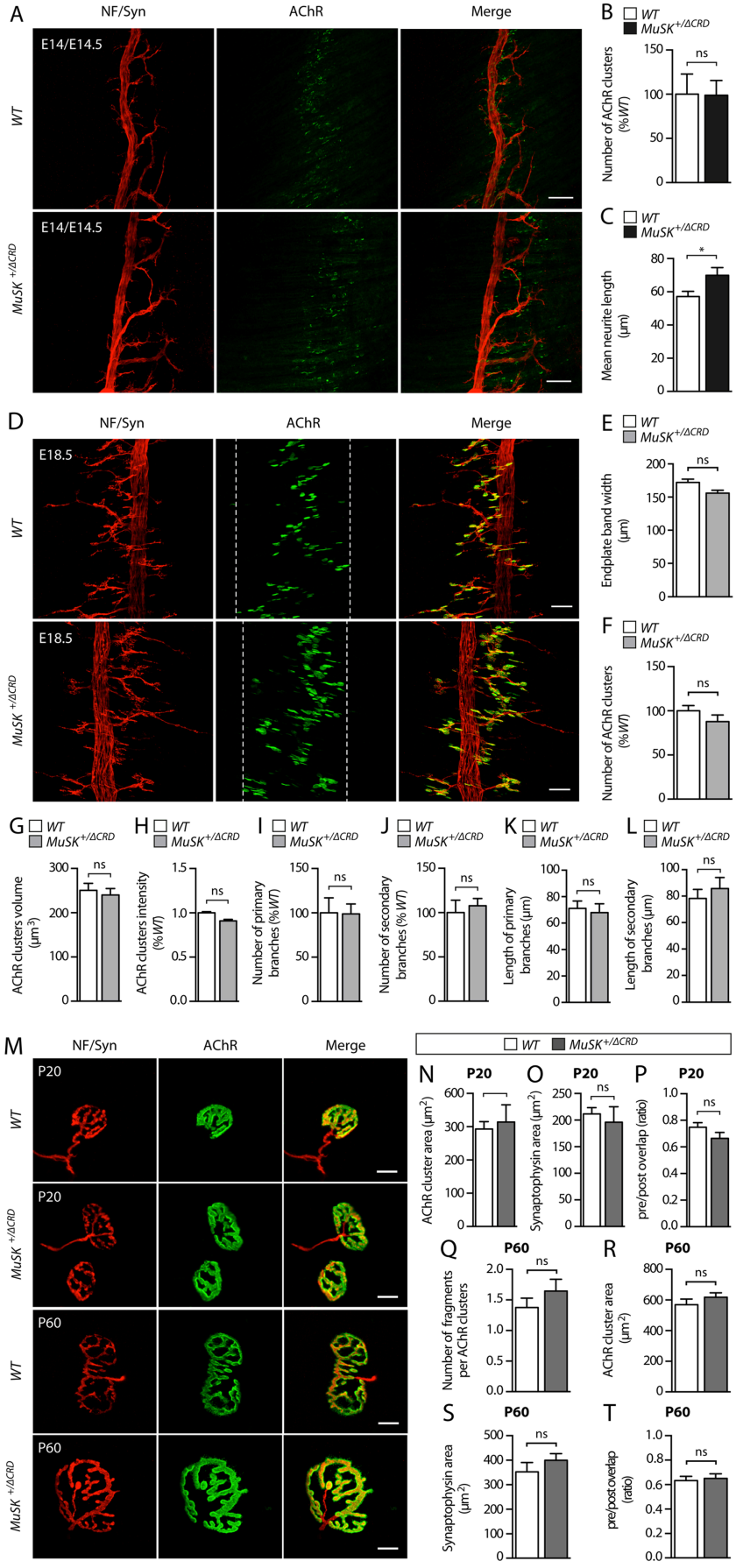


Figure S4.

**Figure S4. Identical NMJ phenotypes between *WT* and *MuSK*$^{+/\Delta CRD}$ mice during synapse formation and maturation.**

**(A)** Confocal images of whole mount left hemidiaphragms from E14/E14.5 *WT* and *MuSK*$^{+/\Delta CRD}$ embryos stained with neurofilament (NF, red) and synaptophysin (Syn, red) antibodies together with α-BTX (green). **(B and C)** Quantitative analysis of the E14/E14.5 AChR clusters number (B) and mean neurite length (C). **(D)** Confocal images of whole mount left hemidiaphragms from E18.5 *WT* and *MuSK*$^{+/\Delta CRD}$ embryos stained as in A. White dashed lines delineate the synaptic endplate band. **(E-L)** Quantitative analysis of the E18.5 endplate band width (E), the AChR clusters number (F), volume (G), fluorescence intensity (H), the number of primary (I) and secondary (J) nerve branches and the mean primary (K) and secondary (L) neurite length. **(M)** Confocal images of whole mount isolated muscle fibers from P20 and P60 *WT* and *MuSK*$^{+/\Delta CRD}$ Tibialis Anterior, stained as in A. **(N-P)** Quantitative analysis of the AChR cluster area (N), the Syn area (O), and overlap area of presynaptic and postsynaptic elements (P) in P20 *WT* and *MuSK*$^{+/\Delta CRD}$ mice. **(Q-T)** Quantitative analysis of the number of fragments per AChR cluster (Q), the AChR cluster area (R), the Syn area (S), and the overlap ratio of presynaptic and postsynaptic elements (T) in P60 *WT* and *MuSK*$^{+/\Delta CRD}$ mice. *$p<0.05$; ns, non significant. Mann-Whitney U test. N=4 embryos or animals per condition. Scale bar in the merged image in A and D, 40 µm; in M, 10 µm.